



Climate engineering by artificial ocean upwelling: Channelling the sorcerer's apprentice

A. Oschlies,¹ M. Pahlow,¹ A. Yool,² and R. J. Matear³

Received 30 November 2009; revised 12 January 2010; accepted 19 January 2010; published 16 February 2010.

[1] Recent suggestions to reduce the accumulation of anthropogenic carbon dioxide in the atmosphere have included ocean fertilization by artificial upwelling. Our coupled carbon-climate model simulations suggest that artificial upwelling may, under most optimistic assumptions, be able to sequester atmospheric CO₂ at a rate of about 0.9 PgC/yr. However, the model predicts that about 80% of the carbon sequestered is stored on land, as a result of reduced respiration at lower air temperatures brought about by upwelling of cold waters. This remote and distributed carbon sequestration would make monitoring and verification particularly challenging. A second caveat predicted by our simulations is that whenever artificial upwelling is stopped, simulated surface temperatures and atmospheric CO₂ concentrations rise quickly and for decades to centuries to levels even somewhat higher than experienced in a world that never engaged in artificial upwelling. **Citation:** Oschlies, A., M. Pahlow, A. Yool, and R. J. Matear (2010), Climate engineering by artificial ocean upwelling: Channelling the sorcerer's apprentice, *Geophys. Res. Lett.*, 37, L04701, doi:10.1029/2009GL041961.

1. Introduction

[2] The rapid and still accelerating increase of atmospheric CO₂ concentrations since the beginning of the industrial revolution is one of the major environmental concerns because of its impact on Earth's radiation budget. While reduction of CO₂ emissions must be the ultimate strategy to address the imminent global warming threat, various carbon sequestration strategies have been proposed to help offsetting our emissions prior to society implementing the necessary infrastructural changes to a much lower CO₂ emission world.

[3] Here we focus on a recent suggestion of using flap-valve operated ocean pipes to upwell nutrient-rich deeper waters in order to fertilize the surface ocean. The intention is to sequester carbon via photosynthetic conversion of dissolved inorganic carbon into organic carbon of which a portion may sink out of the surface layer and thereby be removed from immediate contact with the atmosphere [Lovelock and Rapley, 2007]. A variant of this proposal focuses on enhancing nitrogen fixation by pipe-induced upwelling of excess phosphate [Karl and Letelier, 2008].

[4] Along with the growth-supporting nutrients, upwelled waters will also contain elevated concentrations of dissolved

inorganic carbon [Shepherd *et al.*, 2007]. This feature makes essentially all natural upwelling systems net sources of CO₂ to the atmosphere [Takahashi *et al.*, 1997] and already suggests that artificial upwelling will not everywhere lead to a reduction in surface partial pressure of CO₂ ($p\text{CO}_2$), a necessary condition for enhanced oceanic carbon uptake.

[5] An estimate of the oceanic carbon sequestration potential that could possibly be accessed by ocean pipes can be obtained from observed hydrographic and biogeochemical tracer distributions, assuming that (1) upwelled phosphate and a stoichiometric carbon equivalent (here we use molar C:N = 6.6) are taken up by the marine biota until pre-pipe surface phosphate concentrations are reached, (2) air-sea heat fluxes adjust the temperature of the upwelled water to pre-pipe surface temperatures, and (3) salinity and alkalinity of the upwelled water are mixed conservatively with ambient surface waters. Assumption (1) implies that any nitrate deficits of the upwelled waters are immediately compensated for by nitrogen fixation as implied by the proposal of Karl and Letelier [2008]. The hypothetical pipe-induced surface-water $p\text{CO}_2$ change can then be diagnosed from World Ocean Atlas [Conkright *et al.*, 2002] and Global Data Analysis Project (GLODAP) [Key *et al.*, 2004] data compilations (Figure 1a).

[6] Potential pipe-induced $p\text{CO}_2$ reductions turn out to be largest in the mid-latitude North Pacific and in the subantarctic Southern Ocean where they can reach more than 150 μatm , while there are only small areas in the Atlantic and Indian oceans where ocean pipes could generate a $p\text{CO}_2$ drawdown. In all other regions, artificial upwelling would, under the above assumptions, tend to increase surface water $p\text{CO}_2$. In order to go beyond the relatively simplistic estimates of surface $p\text{CO}_2$ changes, in the following we employ a dynamical coupled carbon-climate model to examine the carbon fluxes predicted by simulated artificial upwelling.

2. Methods

[7] The model used is the University of Victoria (UVic) Earth System Climate Model [Weaver *et al.*, 2001] in the configuration described by Schmittner *et al.* [2008]. The oceanic component is a fully three-dimensional primitive-equation model with nineteen levels in the vertical ranging from 50 m near the surface to 500 m in the deep ocean. It contains a simple marine ecosystem model with the two major nutrients nitrate and phosphate and two phytoplankton classes, nitrogen fixers and other phytoplankton, with the former being limited only by phosphate. This parameterization of nitrogen fixers allows us to account for the recently proposed carbon sequestration by pipe-induced stimulation of nitrogen fixation [Karl and Letelier, 2008]. As a caveat we note that the trace nutrient iron is not explicitly included

¹Leibniz-Institut für Meereswissenschaften an der Universität Kiel (IFM-GEOMAR), Kiel, Germany.

²National Oceanography Centre Southampton, Southampton, UK.

³CSIRO Marine Laboratories, Hobart, Tasmania, Australia.

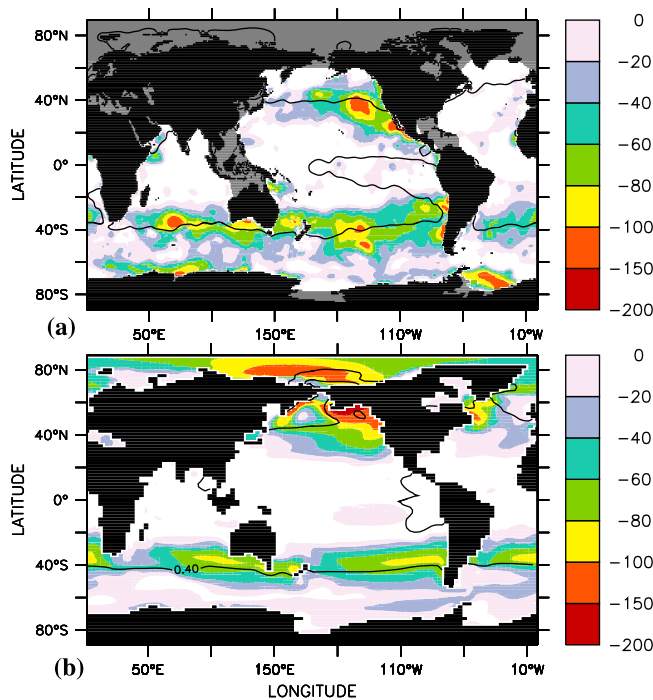


Figure 1. (a) Potential $p\text{CO}_2$ drawdown computed from nutrient, temperature and salinity fields taken from the World Ocean Atlas 2001 (WOA01) [Conkright *et al.*, 2002] and dissolved inorganic carbon (DIC) and alkalinity fields taken from the Global Data Analysis Project (GLODAP) [Key *et al.*, 2004]. The GLODAP data base does not cover the grey shaded areas. (b) Potential $p\text{CO}_2$ drawdown computed from the model output for the simulated year 2100. Units are μatm . The solid line denotes the $0.4 \text{ mmol PO}_4 \text{ m}^{-3}$ isoline at the sea surface. Ocean pipes would lead to a surface-water $p\text{CO}_2$ increase in the white areas. The assumed maximum vertical pipe extension is 1000 m.

in the model, which nevertheless achieves a reasonable fit to observed biogeochemical tracer distributions for the tuned biological parameters and mixing parameterizations [Schmittner *et al.*, 2008; Oschlies *et al.*, 2008]. In particular,

the model can relatively well reproduce observed tracer distributions and air-sea CO_2 fluxes across natural upwelling and downwelling regions, where vertical velocities are often more than an order of magnitude larger than the artificial upwelling velocities applied below.

[8] The ocean component is coupled to a single-level energy-moisture balance model of the atmosphere and a dynamic-thermodynamic sea ice component. The terrestrial vegetation and carbon-cycle component is based on the Hadley Centre's TRIFFID model [Cox *et al.*, 2000]. After a spin up of more than 10,000 years under pre-industrial atmospheric and astronomical boundary conditions, the model is run under historical conditions from year 1850 to 2000 using fossil-fuel and land-use carbon emissions as well as solar, volcanic and anthropogenic aerosol forcings. From year 2000 to 2100, the model is forced by CO_2 emissions following the SRES A2 non-intervention scenario with an increase from today's emissions of about 8 PgC/yr to about 29 PgC/yr in the year 2100.

[9] We simulate the effect of the proposed ocean pipes by introducing artificial transport terms that transfer water from the specified lower end of the pipe to the ocean surface [Yool *et al.*, 2009]. A compensating downwelling velocity at all intermediate levels ensures volume conservation. In areas that contain simulated pipes, water is transferred adiabatically from the grid box at the lower end of the pipe to the surface grid box at a rate of 1 cm/day . For a rough estimate of the required number of pipes, we use a manufacturer's estimate of 1 m diameter pipes pumping up $13 \times 10^3 \text{ m}^3/\text{day}$ [Kithil, 2006]. About one of such pipes would have to be deployed per square kilometer in order to achieve an areal-mean artificial upwelling rate of 1 cm/day . An artificial upwelling rate of 1 Sv ($= 10^6 \text{ m}^3/\text{s}$) would then require about 7 million pipes. We will not further discuss engineering or legal implications of such a pipe array, but in the following only concentrate on their potential feasibility in terms of atmospheric CO_2 reduction and climate impacts. Maximum vertical extensions of the simulated pipes are limited to 1000 m , and sensitivity experiments are run with different maximum pipe extensions and upwelling rates (Table 1). The modeled pipes are installed in the year 2100 and from thereon operate at any water column at any time for which, according to the criteria described above, a pipe-induced

Table 1. Model Simulations^a

Experiment	$p\text{CO}_2$ (μatm)	C_{atm} (PgC)	C_{oc} (PgC)	C_{ter} (PgC)	SAT ($^{\circ}\text{C}$)	EP ($\frac{\text{PgC}}{\text{yr}}$)	Upwell (Sv)	N_2 Fix ($\frac{\text{TmolN}}{\text{yr}}$)
<i>Control, SRES 92A Emission Scenario</i>								
A.D. 1765	280	574	37343	1928	13.01	7.0		140
A.D. 2010	385	788	37492	2094	13.85	6.8		136
A.D. 2100	866	1772	37861	2405	16.49	6.3		129
<i>Pipe Minus Control, Year 2100, Different Maximum Pipe Extensions</i>								
$1 \frac{\text{cm}}{\text{day}}$, 1000m	-41	-83	18	66	-0.83	3.4	26.4	122
$1 \frac{\text{cm}}{\text{day}}$, 500m	-30	-62	10	53	-0.63	2.9	25.2	110
$1 \frac{\text{cm}}{\text{day}}$, 250m	-13	-27	4.5	23	-0.29	1.0	16.3	4.1
$1 \frac{\text{cm}}{\text{day}}$, 130m	-1.8	-2.4	-0.8	3.2	-0.058	0.17	11.0	4.9
<i>Pipe Minus Control, Year 2100, Different Upwelling Velocities</i>								
$0.05 \frac{\text{cm}}{\text{day}}$, 1000m	-2.4	-5.0	0.16	4.8	-0.057	0.22	1.44	8.3
$0.1 \frac{\text{cm}}{\text{day}}$, 1000m	-5.6	-11.5	2.1	9.4	-0.12	0.43	2.86	17
$0.5 \frac{\text{cm}}{\text{day}}$, 1000m	-26	-54	15	40	-0.52	2.0	13.8	75
$5 \frac{\text{cm}}{\text{day}}$, 1000m	-53	-109	-7.9	118	-1.41	5.8	101	172

^aAll experiments use the SRES A2 emission scenario, pipe experiments are referred to by the artificial upwelling velocity and the maximum vertical extent of the pipes. C_{atm} , C_{oc} , and C_{ter} are atmospheric, oceanic, and terrestrial carbon inventories, SAT is the global mean surface air temperature, EP is the export of organic carbon across $z = 125 \text{ m}$, upwell is the pipe induced upwelling in $\text{Sv} = 10^6 \text{ m}^3/\text{s}$, and N_2 fix is nitrogen fixation.

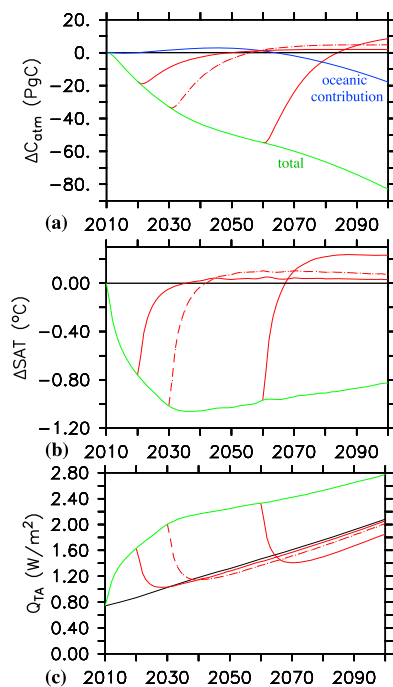


Figure 2. (a) Simulated sequestration of atmospheric CO₂ relative to the standard run without pipes. (b) Simulated surface air temperature difference of ocean pipe simulation relative to the standard run without pipes. (c) Simulated radiation balance at the top of the atmosphere. Green lines refer to the standard pipe experiment with pipes deployed wherever a reduction in surface $p\text{CO}_2$ can be expected, and with a maximum vertical pipe extension of 1000 m. Red lines show results from simulations with artificial upwelling stopped after 10, 20, and 50 years, respectively. The blue line in Figure 2a denotes carbon sequestration due to oceanic uptake, the black line in Figure 2b refers to the control experiment without pipes.

local reduction in surface $p\text{CO}_2$ can be expected. We impose an additional condition that simulated pipes are not installed in areas with surface phosphate concentrations exceeding 0.4 mmol m^{-3} . Such areas do not appear to suffer from phosphate limitation, and our first assumption of a drawdown of piped-up nutrients to pre-pipe nutrient levels may not be valid. Figure 1b shows the situation for the simulated year 2010. It agrees with the observational estimate in the location of the main areas favorable for ocean pipes, namely the subantarctic Southern Ocean and the North Pacific (the Arctic Ocean is not covered by the GLODAP data base).

3. Results

[10] For the standard pipe experiment with 1 cm/day artificial upwelling from a maximum depth of 1000 m the simulated artificial upwelling of all pipes taken together is about 20 Sv in year 2010. With vertical gradients of anthropogenic CO₂ increasing with time, the area suitable for artificial upwelling also gets larger, and simulated artificial upwelling reaches a global value of 26 Sv in year 2100 (Table 1). Compared to the control experiment, the pipe-induced upwelling leads to an overall increase in the strength

of the meridional overturning circulation by up to 30%, which counteracts the 20% decline in overturning strength experienced by the control run under global warming over the 21st century [Schmittner *et al.*, 2008]. The stronger overturning in the pipe experiment enhances the upwelling of deeper waters generally rich in CO₂ and thereby partly compensates the fertilization-induced carbon drawdown.

[11] As expected, pumping up nutrients into the otherwise nutrient-depleted upper ocean results in a significant enhancement of biological production, which may have benefits such as enhancing mariculture [Liu *et al.*, 1999]. Annual export of organic matter across a depth level of 125 m increases from 6.3 PgC/yr in the control run by more than 50% to 9.7 PgC/yr in the artificial upwelling run (Table 1). This includes the contribution from nitrogen fixation, which for the model's simple parameterization in terms of excess phosphate almost doubles from 129 Tmol N/yr to 251 Tmol N/yr when pipes are implemented. This corresponds to an additional carbon fixation of 0.7 PgC/yr. Despite the substantial increase in the export of organic carbon, the cumulative oceanic carbon sequestration amounts to only 18 PgC by year 2100, which is about 7% of the cumulative increase in export production. About 70% of the exported carbon returns to the atmosphere on a centennial time scale because of shallow remineralisation [Oschlies, 2009], and a smaller CO₂ backflux arises from the enhanced upwelling of carbon-rich deeper waters in the standard pipe run. Ecological impacts, e.g. of enhanced shallow remineralization, are difficult to predict and may feed back on biogeochemical cycles in ways not accounted for by the current model.

[12] An unexpected result evident in all pipe runs is a reduction in atmospheric CO₂ that is much larger than the increase in the oceanic carbon inventory (Figure 2a and Table 1). In the standard pipe run the reduction in atmospheric CO₂ compared to the control run has, by year 2100, reached 83 PgC or 41 μatm , i.e., more than four times the oceanic sequestration. Thus, in our model about 80% of the carbon sequestered from the atmosphere enters the terrestrial carbon pool. The reason for the pipe-induced enhancement in terrestrial carbon storage is the temperature sensitivity of the terrestrial carbon pools. Artificial upwelling leads to colder sea surface waters, which cool the overlying air and, eventually, the continental soils. As shown in Figure 2b, simulated global surface air temperatures drop by up to 1°C with respect to the control run within the first decades of the pipes operating. Lower temperatures decrease terrestrial net primary production and, to a larger extent, heterotrophic respiration in vegetation and soils in our model. The net effect is an increase in the terrestrial carbon pool in the artificial upwelling run compared to the control simulation (Table 1).

[13] In the carbon-climate model used here, the climate sensitivity of the modeled terrestrial carbon pool is in the middle range of the Coupled Climate–Carbon Cycle Model Intercomparison Project (C⁴MIP) models [Friedlingstein *et al.*, 2006]. Even for a climate sensitivity at the low end of the C⁴MIP range, the upwelling-induced cooling would still generate a terrestrial carbon uptake as large as the simulated oceanic uptake.

[14] A second unexpected result is that conditions do not simply revert to those of the control run when artificial upwelling is stopped. In contrast to other climate engineering

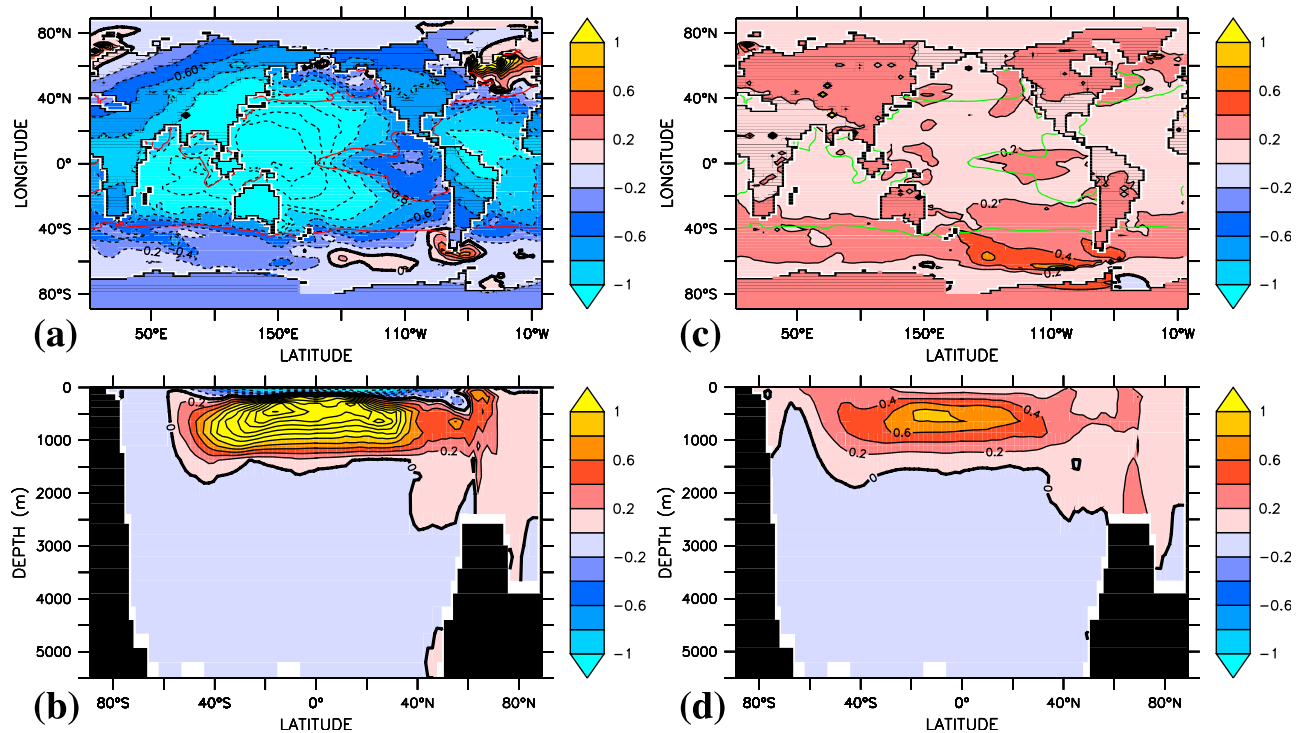


Figure 3. (a) Simulated year-2100 surface temperature difference and (b) zonally averaged temperature difference between the standard pipe experiment and the control run without ocean pipes. The red contour in Figure 3a denotes the region covered by ocean pipes in year 2100. (c) Simulated year-2100 surface temperature difference and (d) zonally averaged temperature difference between the run with pipes operating for 50 years before being turned off in year 2060 and the control run that never experienced ocean pipes. The green contour in Figure 3c denotes the region covered by ocean pipes in year 2060.

proposals [e.g., *Matthews and Caldeira, 2007*], both surface temperature and atmospheric CO_2 rise to levels even higher than those of the control experiment (Figure 2). In year 2100 simulated temperatures are higher than those of the control run by 0.03°C , 0.07°C , and 0.23°C when artificial upwelling is stopped after 10, 20, and 50 years, respectively. Though small compared to the 2.6°C temperature increase simulated by the control run by year 2100 (Table 1), an extra warming would pose an additional threat to ecosystems and society.

[15] The explanation for the extra warming is an artificial-upwelling induced perturbation of the planet's heat budget: Upwelling tends to lower surface temperatures (Figure 3a). Besides mitigating global warming, this might weaken the intensity of tropical storms [*Webster et al., 2005*] not resolved by our model. However, a colder surface of the planet will also emit less thermal radiation back into space. In our standard pipe experiment the net downward radiation flux at the top of the atmosphere increases by about 0.8 W/m^2 during the operation of the ocean pipes, i.e., it approximately doubles with respect to the global warming run without ocean pipes (Figure 2c). By lowering surface temperatures, simulated artificial upwelling thus leads to an additional heat uptake of the planet, with the extra heat stored predominantly in the ocean's low-latitude subsurface waters (Figure 3b). Once artificial upwelling stops, this extra heat makes its way back to the sea surface on the decadal time scale of the thermocline ventilation. Surface warming is most intense along the poleward margins of the subtropical gyres where thermocline waters are entrained into the surface mixed layer (Figures 3c

and 3d). The elevated surface temperatures then allow radiating the extra heat back into space (Figure 2c).

4. Conclusions

[16] Our study suggests that artificial upwelling by ocean pipes may, under the hypothetical and most optimistic assumption of a massive deployment of perfect ocean pipes, be able to sequester atmospheric CO_2 at a rate of about 0.9 PgC/yr , approximately corresponding to one “stabilization wedge” [*Pacala and Socolow, 2004*]. Interestingly, most of the carbon sequestered from the atmosphere by artificial ocean upwelling is, in our model, stored on land and not in the ocean. The dominance of carbon storage on land is consistently found in all our sensitivity experiments assuming different deployment numbers and different designs of ocean pipes, as well as for the wide range of climate sensitivities of the terrestrial carbon pools in the C^4MIP models [*Friedlingstein et al., 2006*], for which we estimate total sequestration rates from half as large to twice as large as in our standard simulation. While this non-local impact of ocean pipes makes it extremely challenging to monitor and evaluate success or failure of such a hypothetical carbon sequestration option, our model simulations predict another caveat:

[17] When upwelling is stopped for whatever reasons, both surface temperatures and atmospheric CO_2 levels rise to levels even somewhat higher than in a world that had never engaged in artificial upwelling. This is because artificial upwelling is expected to further increase the imbalance

of the planetary radiation budget. It may thereby limit the options for action of future generations.

[18] **Acknowledgments.** We thank John Shepherd and two anonymous reviewers for helpful comments on earlier versions of the manuscript and are grateful for the support from Mike Eby from the UVic model support team. A.O. thanks Eberhard Fudickar for drawing attention to this topic.

References

- Conkright, M. E., H. E. Garcia, T. D. O'Brien, R. A. Locarnini, T. P. Boyer, C. Stephens, and J. I. Antonov (2002), *World Ocean Atlas 2001, vol. 4, Nutrients, NOAA Atlas NESDIS*, vol. 54, 392 pp., NOAA, Silver Spring, Md.
- Cox, P. M., R. A. Betts, C. D. Jones, S. A. Spall, and I. J. Totterdell (2000), Acceleration of global warming due to carbon-cycle feedbacks in a coupled climate model, *Nature*, *408*, 184–187.
- Friedlingstein, P., et al. (2006), Climate-carbon cycle feedback analysis: Results from the C4MIP model intercomparison, *J. Clim.*, *19*, 3337–3353.
- Karl, D. M., and R. M. Letelier (2008), Nitrogen fixation-enhanced carbon sequestration in low nitrate, low chlorophyll seascapes, *Mar. Ecol. Prog. Ser.*, *364*, 257–268.
- Key, R. M., A. Kozyr, C. L. Sabine, K. Lee, R. Wanninkhof, J. L. Bullister, R. A. Feely, F. J. Millero, C. Mordy, and T.-H. Peng (2004), A global ocean carbon climatology: Results from Global Data Analysis Project (GLODAP), *Global Biogeochem. Cycles*, *18*, GB4031, doi:10.1029/2004GB002247.
- Kithil, P. (2006), A device to control sea surface temperatures and effects on hurricane strength, *EOS Trans. AGU*, *87*, Ocean Sci. Meet. Suppl., Abstract OS25C-10.
- Liu, C. C. K., J. J. Dai, H. S. Lin, and F. Guo (1999), Hydrodynamic performance of wave-driven artificial upwelling device, *J. Eng. Mech.*, *125*, 728–732.
- Lovelock, J. F., and C. G. Rapley (2007), Ocean pipes could help the Earth to cure itself, *Nature*, *449*, 403.
- Matthews, H. D., and K. Caldeira (2007), Transient climate-carbon simulations of planetary geoengineering, *Proc. Natl. Acad. Sci. U. S. A.*, *104*, 9949–9954.
- Oschlies, A. (2009), Impact of atmospheric and terrestrial CO₂ feedbacks on fertilization-induced marine carbon uptake, *Biogeosciences*, *6*, 1603–1613.
- Oschlies, A., K. G. Schulz, U. Riebesell, and A. Schmittner (2008), Simulated 21st century's increase in oceanic suboxia by CO₂-enhanced biological carbon export, *Global Biogeochem. Cycles*, *22*, GB4008, doi:10.1029/2007GB003147.
- Pacala, S., and R. Socolow (2004), Stabilization wedges: Solving the climate problem for the next 50 years with current technologies, *Science*, *305*, 968–972.
- Schmittner, A., A. Oschlies, H. D. Matthews, and E. D. Galbraith (2008), Future changes in climate, ocean circulation, ecosystems and biogeochemical cycling simulated for a business-as-usual CO₂ emission scenario until 4000 AD, *Global Biogeochem. Cycles*, GB1013, doi:10.1029/2007GB002953.
- Shepherd, J. G., D. Iglesias-Rodríguez, and A. Yool (2007), Geo-engineering might cause, not cure, problems, *Nature*, *449*, 781.
- Takahashi, T., R. A. Feely, R. F. Weiss, R. H. Wanninkhof, D. W. Chipman, S. C. Sutherland, and T. T. Takahashi (1997), Global air-sea flux of CO₂: An estimate based on measurements of sea-air pCO₂ difference, *Proc. Natl. Acad. Sci. U. S. A.*, *94*, 8292–8299.
- Weaver, A. J., et al. (2001), The UVic Earth system climate model: Model description, climatology, and applications to past, present and future climates, *Atmosphere Ocean*, *39*, 361–428.
- Webster, P. J., G. J. Holland, J. A. Curry, and H.-R. Chang (2005), Changes in tropical cyclone number, duration, and intensity in a warming experiments, *Science*, *309*, 1844–1846.
- Yool, A., J. G. Shepherd, H. L. Bryden, and A. Oschlies (2009), Low efficiency of nutrient translocation for enhancing oceanic uptake of carbon dioxide, *J. Geophys. Res.*, *114*, C08009, doi:10.1029/2008JC004792.

R. J. Matear, CSIRO Marine Laboratories, Hobart, Tas 7000, Australia. (richard.matear@csiro.au)

A. Oschlies and M. Pahlow, Leibniz-Institut für Meereswissenschaften an der Universität Kiel (IFM-GEOMAR), Düsternbrooker Weg 20, D-24105 Kiel, Germany. (aoschlies@ifm-geomar.de; mpahlow@ifm-geomar.de)

A. Yool, National Oceanography Centre Southampton, European Way, Southampton SO14 3ZH, UK. (axy@noc.soton.ac.uk)